Home   Search   Collections   Journals   About   Contact us   My IOPscience

Humidity effect of domain wall roughening behavior in ferroelectric copolymer thin films

Humidity effect of domain wall roughening behavior in ferroelectric copolymer thin films

Kwang-Won Park[1], Hosung Seo[2], Jiyoon Kim[1], Daehee Seol[2], Jongin Hong[1] and Yunseok Kim[2]

[1] Department of Chemistry, Chung-Ang University, Seoul 156-756, Republic of Korea
[2] School of Advanced Materials Science and Engineering, Sungkyunkwan University, Suwon, Gyeonggi-do 440-746, Republic of Korea

E-mail: hongj@cau.ac.kr and yunseokkim@skku.edu

Abstract

We have demonstrated that domain switching in ferroelectric copolymer films can be significantly affected by humidity. With increasing relative humidity (RH), we observed larger domains with highly irregular boundaries as a result of lateral spreading of the tip-induced electric field that originates from water adsorption. Fractal dimension study of irregular domains reveals that the fractal dimension is higher in cases where the RH is higher. The results show that the RH is one of the major switching parameters in ferroelectric copolymers, and therefore could allow clear understanding with regard to domain switching behavior in the ferroelectric copolymer films under ambient conditions.

Keywords: ferroelectric copolymer, piezoresponse force microscopy, humidity, P(VDF-TrFE), fractal dimension

(Some figures may appear in colour only in the online journal)

Introduction

Organic ferroelectric materials have many highly desirable practical applications, such as nonvolatile memories, radio-frequency identification tags, piezoelectric energy harvesters, and photovoltaic devices [1–7]. Among various organic ferroelectric materials, poly(vinylidene fluoride-co-trifluoroethylene) P(VDF-TrFE) copolymers are definitely notable not only for their large remnant polarization, but also for their fast switching time, low processing temperature, and flexibility [8, 9]. Accordingly, ferroelectric copolymers have been investigated specifically in terms of their ferroelectric switching, since the control of ferroelectric polarization is essential for applications. One of the classic ways to explore ferroelectric switching is a scanning probe microscopy-(SPM) based method known as piezoresponse force microscopy (PFM). PFM is based on the detection of polarization status through the cantilever deflection that originates from the piezoelectric response of ferroelectric materials. PFM allows us to explore ferroelectric domain structures and switching behavior at the nanoscale; switching behaviors in

the ferroelectric copolymer studied by PFM have been reported by some researchers [1, 10–12].

However, previous reports primarily focused on the electric-field-induced effect on switching behavior. In fact, since ambient conditions including humidity, gas, and temperature could have tremendous influence on the ferroelectric properties, their effects on the ferroelectric properties (i.e., switching behavior) should be taken into account with respect to the aforementioned applications. In particular, water can adsorb on the film surface under ambient conditions. The adsorbed water layer can affect polarization switching behavior, and thus it can play a crucial role in ferroelectric performance. Indeed, a great deal of research has been carried out by means of SPM to understand the ferroelectric properties associated with water [13–15]. The presence of water at the interface between a tip and a sample surface greatly influences material properties as well as switching circumstances using SPM. Since the capillary condensation of water in the gap between the tip and the sample surface cannot be neglected [16], humidity can affect the sizes of switched domains in the ferroelectric oxides [17–20]. Accordingly, humidity could affect the reliability of written bits in the

ferroelectric polymer-based memory devices. However, if we can control the humidity effect, we can reduce electrical power needed for writing bits in the memory devices, because humidity affects the domain size. While humidity is one of the most important parameters for ferroelectric switching even in the ferroelectric copolymer, humidity's effect on domain shape and domain wall roughness has not, up to now, been fully understood.

Here, we use PFM measurements to demonstrate that humidity can significantly affect switching behavior in the P(VDF-TrFE) thin films. In particular, humidity dependent domain geometry, which can be evaluated by fractal dimension analysis, is investigated in the ferroelectric copolymer thin films. The results show that fractal dimension values are strongly dependent on relative humidity (RH) rather than on other factors.

Experimental setup

A ferroelectric random copolymer consisting of 75% vinylidene fluoride and 25% trifluoroethylene (75:25 copolymer) with a molecular weight of 200 000 was used, and its pellets were dissolved in methyl ethyl ketone to prepare a $2.5 \, \mathrm{g \, L^{-1}}$ concentration. The solution was spin-coated onto Pt/Ti/SiO$_2$/Si substrates at 5000 rpm for 20 s using a spin-coater (ACE-2000, Dong-Ah Trade Corp., Korea). The spin-coated P(VDF-TrFE) film was then annealed on a hot plate at 130 °C for 12 h to ameliorate its crystallinity and remove residual solvent. The P(VDF-TrFE) film was 100 nm thick, as determined by transmission electron microscopy after cross-sectional specimens were prepared by a focused ion beam. The crystallinity and molecular conformations of the films were analyzed using a x-ray diffractometer (XRD, X'Pert Pro MRD, PANalytical, Netherlands) and a Fourier transform infrared (FTIR) spectrometer (Vertex 80, Bruker Optics, Germany) with an image microscope (Hyperion 3000, Bruker Optics, Germany), respectively.

A commercial atomic force microscope (AFM, XE-120 and NX-10, Park Systems, Korea) equipped with a lock-in amplifier (SR830, Stanford Research Systems, USA) was used to analyze ferroelectric domain structures. An ac modulation voltage of 2 V_{rms} at 17 kHz [12] was applied to a Pt/Ir-coated Si tip (PPP-CONTPt, Nanosensors, Swiss, force constant k ≈ 0.2 N m^{-1}), and this enabled the measurement of electrical and topological properties both simultaneously and independently. Local piezoresponse hysteresis loops were measured over 25 different locations. PFM images were taken by scanning $1.5 \, \mu\mathrm{m} \times 1.5 \, \mu\mathrm{m}$ with 256×256 pixels at every domain. The RH in the chamber was controlled from 15% to 70% by a humidifier to observe the effect of the humidity on the domain size. A digital thermohygrometer (608-H2, Testo, Germany) with ±2% RH accuracy was used to detect humidity. The size and perimeter of each domain was analyzed by XEI software (Park Systems, Korea)−a commercial image processing program for AFM data−to determine the spatial disorder of the ferroelectric medium under different humidity conditions.
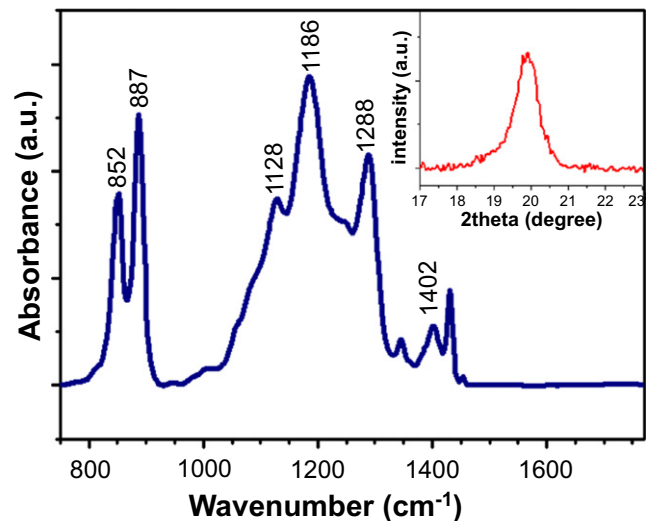

Figure 1. FTIR spectra of P(VDF-TrFE) (75:25) film. From the dominant peaks at 852 cm^{-1} and 1288 cm^{-1}, we could verify that the film had a good crystalline ferroelectric β-phase. The inset shows the XRD data, which confirm its crystallinity.

Results and discussion

In the FTIR spectrum (figure 1), the absorption bands at 1288 cm^{-1} and 852 cm^{-1} (A$_1$, $\mu \| b$) are associated with ferroelectric β-phase possessing *trans* sequences longer than four monomers ($t_m > 4$) and *trans* sequences longer than three monomers ($t_m > 3$), respectively [21]. Absorption bands at 1186 cm^{-1} and 887 cm^{-1} (B$_2$, $\mu \| a$) are related to antisymmetric CF$_2$ stretching vibrations and *trans* sequences of one monomer. In the inset of figure 1, we see the prominent XRD peak at $2\theta = 19.7°$, which stems from (110) and (200) reflection of the crystalline β-phase. What arouses our interest is that spin-casted films show that the carbon chains are predominantly parallel to the substrate, since hydrodynamic flow stretches them [22]. This can be confirmed by the absorption peak parallel to either the *a*- or *b*-axis in the FTIR analysis, and by the (110) peak at around 20° in the XRD.

We first examined basic switching behavior using a piezoresponse hysteresis loop. As we see in figure 2, a well-defined hysteresis loop was obtained by PFM. Interestingly, asymmetric behavior was observed in the coercive voltages. While the positive coercive voltage is +9.8 V, the negative coercive voltage is −11.3 V. In addition, the topography image of the P(VDF-TrFE) thin films in the inset of figure 2 shows a smooth surface, of which roughness is about 2.0 nm.

We further examined switching behavior by applying a bias pulse after background poling by scanning with −15 V for positively switched domains (+15 V for negatively switched domains) at a constant RH condition of about 30%. Through this method, we found that penetrated domains through the thickness direction can be generated by applying at least 13 V with 50 ms of pulse width. Here, we examined switching behavior under electric field conditions only for the fully penetrated domains, which can be ascertained by the PFM phase and amplitude images [23]. Figures 3(a) and (b) illustrate PFM phase images of switched domains induced by
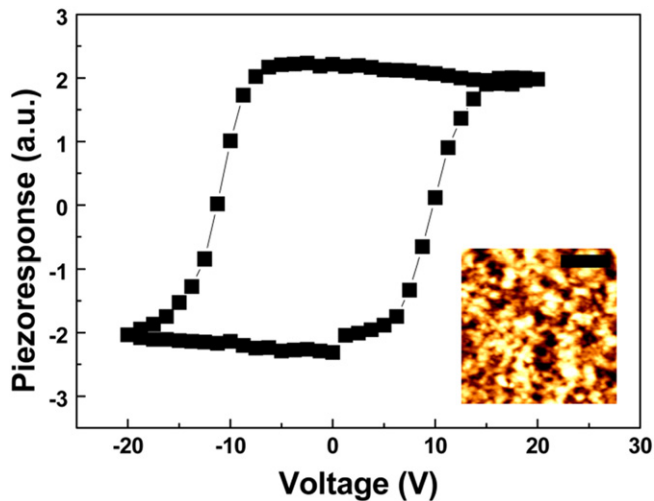
Figure 2. Piezoresponse hysteresis loop measured by PFM, which was averaged over 25 different locations. Inset shows topography image of the P(VDF-TrFE) film. Scale bar is 500 nm.
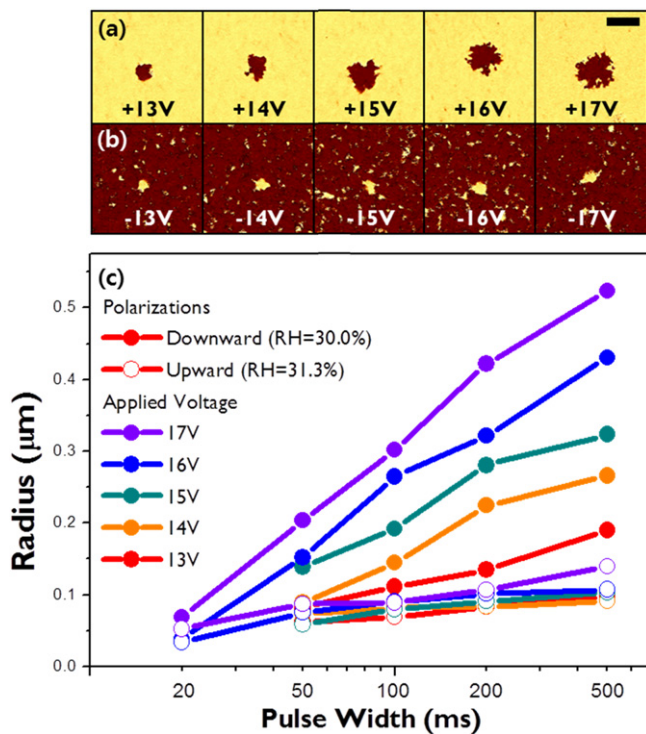

Figure 3. PFM phase images of the voltage-amplitude-dependent domain structures: (a) tip-induced positive bias and (b) negative bias at 30% and 31.3% RH, respectively (pulse width was fixed at 100 ms). Background poling was performed by scanning with a −15 V dc tip bias for (a) and a +15 V bias for (b) prior to the domain switching process. Scale bar is 500 nm. (c) Plot of domain radius versus logarithmic pulse width of the downward (solid circles) and upward (hollow circles) domains under different voltage conditions with increasing pulse width from 20 ms to 500 ms and voltage from ±13 to 17 V.

bias pulses with a fixed pulse width of 100 ms. Downward domains show that domain growth is linearly proportional to the logarithmic value of pulse width, similar to the domain radius behavior in the previous report [12]. Even though the

upward domains seem to follow similar behavior, it is rather unclear because the incremental changes are very small. As shown in figure 3(c), downward domains induced by positive bias pulses (+13 to +17 V, 100 ms) show larger switched areas than the upward domains induced by negative bias pulses (−13 V to −17 V, 100 ms). This asymmetric switching comes from the wide distribution of internal self-polarized regions between the ferroelectric film and the bottom electrode attributed to align dipoles, which is also known as band bending at the film-electrode interface. This negative pinning implies that, if the absolute magnitude of bias voltage is the same, positive bias can more easily switch domains than negative bias. This phenomenon could also originate from a Schottky barrier between a ferroelectric copolymer thin film and a metal bottom electrode [12, 24]. Indeed, as mentioned before, asymmetric behavior on the coercive voltage was observed in the hysteresis loop of figure 2. This is consistent with the obtained switching results in figure 3. Even though one would expect that work function differences between top and bottom electrodes could be one of the potential causes, we can exclude it as a reason because the top and bottom electrodes are the same material. The topmost layer of the bottom electrode and the AFM tip are both coated with Pt, so asymmetric polarization could be caused primarily by the band-bending effect between the film and electrode interface because the work function difference is zero [25, 26].

Interestingly, some of the downward domains in figure 3(a) show highly irregular domain walls. It has been well known that spin-coated P(VDF-TrFE) is not only heavily imprinted, but also has local structural disorder potential [27, 28]. Sharma et al have also reported that ferroelectric polymer thin film has a strong affinity toward downward polarity in terms of asymmetric random-field disorder [29]. This disorder gives rise to the phenomenon of irregular domain walls with asymmetric switching. Nevertheless, we speculate that the irregular domain walls could be affected by external influences (e.g., ambient conditions).

To study the irregular domain wall, we performed switching experiments at different RH conditions. As figure 4 clearly shows, it was found that the switched area and the perimeter of the downward domains increase under increasing RH conditions. Furthermore, the domain walls seem to be more irregular at higher RH conditions. Since domain perimeter values are more vulnerable to changing RH than radius values, perimeter values of each domain are randomly chosen and denoted on the graph in figure 4(b). We can then conclude that the domain irregularly grows faster when the sample is exposed to moister conditions. The two following hypotheses can explain the observed phenomena: First, the adsorbed water on the junction area between the tip and the sample leads to different sizes of meniscus, according to the RH conditions [17]. Second, water is regarded as a good conducting material to propagate the electric field well, even in the gas phase [30]. Under very humid conditions, considerable meniscus at the tip/sample junction could enable the lateral augmentation of the electric field area. Thus, the spatial area of the tip-induced field, which can be increased by the
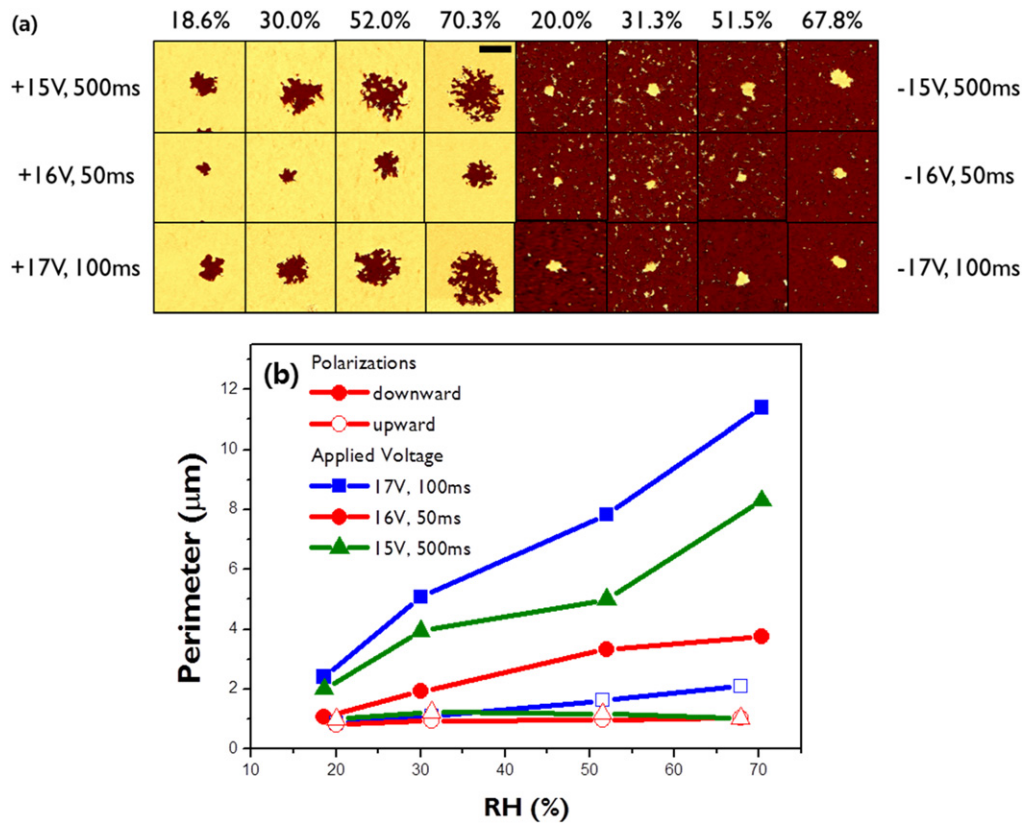
Figure 4. (a) PFM phase images of the downward and upward domains at different RH conditions. Pulse amplitude and width were ±15 V and 500 ms, ±16 V and 50 ms, and ±17 V and 100 ms from the first row of the images, respectively. Scale bar is 500 nm. (b) Dependence of the perimeter of the downward (solid) and upward domains (hollow) on the RH conditions. Each point represents the domains in (a). Applied voltage conditions are denoted in the legend.

RH factor, results in remote nucleation and highly irregular domain walls, particularly for downward domains. In addition, there are disordered defects that lead to domain wall roughening. Thus, the larger the domain increases, the more irregular domain boundaries can be seen, yielding larger perimeter values with increasing RH conditions. On the other hand, irregular domain walls can be partially correlated with morphology of the films [31]. However, since highly irregular domain walls under high RH conditions cannot originate solely from the morphology, this cannot be a major effect on the formation of irregular domain walls.

However, similar to the asymmetric switching by the application of electric field seen in figure 3, asymmetric behavior was also observed in figure 4. In other words, the switching behavior of the upward domains is less sensitive to RH conditions. Since RH conditions can be a major switching parameter, strong imprint—which was discussed before—can be a possible reason for the observed asymmetric behavior as well. We further note that the humidity's influence on switching behavior shows reversible behavior.

Although domain area analysis is a typical way to investigate domain growth behavior, perimeter analysis of every domain is an essential prerequisite for heavily irregularly shaped domain walls. Thus, to further explore the irregular domain wall, we performed fractal dimension analysis of individual domains (figure 5) which allows us to

characterize the evolution of the domain geometry in the switching process [28, 30, 32]. The fractal dimension (or Hausdorff constant) is derived from the log–log plot of the domain perimeter, P, versus area, A: $P = K \cdot A^{D/2}$ where K is a prefactor and D is dimensionality (see figure 5(a)). Its slope provides the degree of spatial disorder of the given domains. In two-dimensional surfaces, a circular domain with perfectly smooth boundaries has a fractal dimension value of approximately one ($D = 1$), while extremely irregular domains have a fractal dimension value of approximately two ($D = 2$). It was reported that the fractal dimensions of the P(VDF-TrFE) films made by spin-coating or the Langmuir-Blodgett method yielded a value, D, of ~1.32 for the irregular downward domains [27, 29], which was lower than that of the ferroelectric oxides [33, 34]. We, however, found results that fractal dimension values varied under different RH environments in the case of downward domains. In other words, the domain wall becomes more irregular when the humidity is higher. As we can see in figure 5, the fractal dimension of the downward domains varied from $D = 1.22$ to 1.53, corresponding to variation of RH conditions at 18.6% and 70.3%, respectively. This suggests that humidity has a critical role in domain-switching dynamics in ferroelectric copolymers. In contrast to the fractal dimension of the downward domains linearly increasing with increasing RH, fractal dimension values for the upward domains show similar values of fractal
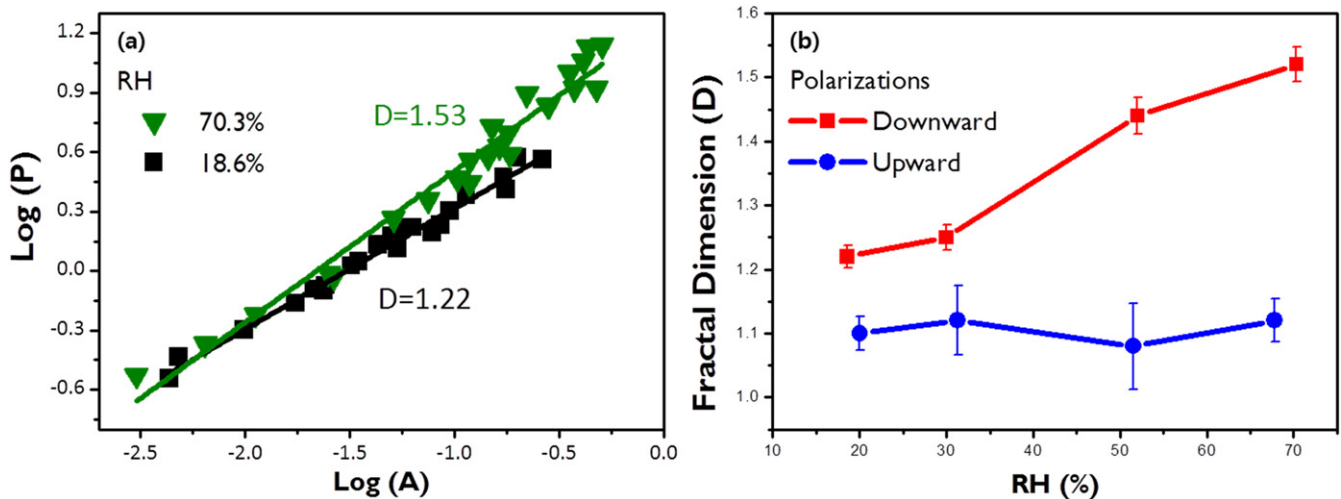
Figure 5. (a) Log–log plot of perimeter versus area in the downward domains at 18.6% (black, square) and 70.3% (green, inverse triangle) RH, respectively. The solid lines, which are the fractal dimension, are linearly fitted curves of the experimental data set. (b) Fractal dimensions of the downward domains (red square) and upward domains (blue circle) at each RH environment (its range is from 18.6 to 70.3%). The solid lines are guides for the eye. Fractal dimensions are acquired from domains switched by bias pulses of ±13, 14, 15, 16, and 17 V with pulse widths of 50, 100, 200, and 500 ms. Error bar means standard errors from every dimension of 20 to 23 domains at each RH condition.
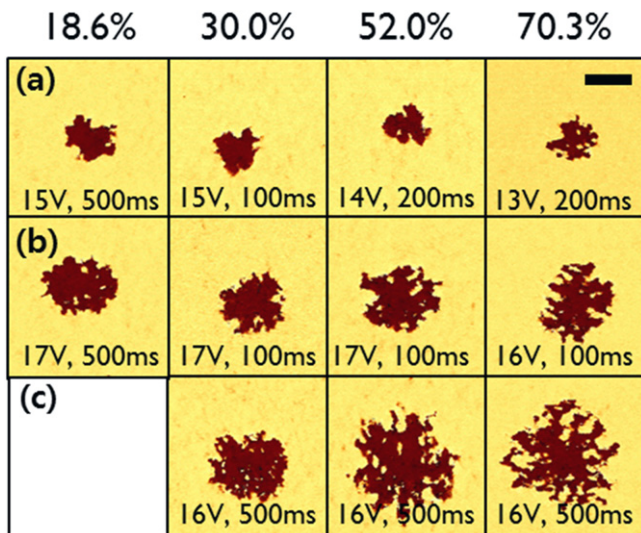

Figure 6. The PFM phase images of the downward domains (a)–(c) in each row have approximately the same domain areas with different humidity, pulse width, and amplitude conditions. Domain areas are (a) $1.10 \pm 0.05\ \mu m^2$, (b) $2.84 \pm 0.03\ \mu m^2$, and (c) $5.41 \pm 0.41\ \mu m^2$. Scale bar is 500 nm.

dimension (i.e., $D \sim 1.12$) for overall RH conditions. The obtained asymmetric behavior on the polarity is consistent for different analyses and consequently, the fractal dimension of the upward domains is not significantly affected by RH conditions. Note that there can be an uncertainty in the perimeter values for small domains due to the resolution of the images. Accordingly, this might affect the accuracy of the fractal dimension, but it might not significantly affect the tendency of the fractal dimension to depend on the humidity. In addition, in figure 6, we can clearly see how water molecules work well as a 'domain spreader.' We have chosen three sets of domains which have similar areas under different RH

conditions. The similar area can be achieved by applying smaller or shorter bias pulses under higher RH conditions (see figures 6(a) and (b)). This clearly shows that humidity can be a major switching parameter. Furthermore, it is feasible that we can reduce the switching power by controlling humidity. Although these domains have analogous areas, the domain shape under each RH condition appears to be different because of irregular domain boundaries. In particular, the larger area shows more irregular domain boundaries (see figure 6(c)). This means that, even if the genuine area of each domain can be preserved, the effective area, which is domain radii, can be spread by the RH environment, inducing an increase in the domain growth rate. Again, this reveals that such humidity effects can also be a major switching parameter in both the ferroelectric polymers and the electric field.

Conclusions

In conclusion, we have investigated humidity's effect on switching behavior in ferroelectric copolymer film using PFM measurements. Interestingly, highly irregular domain boundaries were observed in the downward domains, owing to their imprint property. We further observed that domain walls become more irregular and larger in a higher-RH environment. The obtained results indicate that, in addition to the electric field, humidity can also be a significant factor on domain switching in ferroelectric copolymer thin films.

Acknowledgments

References

[1] Brian J R, Jesse S, Kalinin S V, Kim J, Ducharme S and Fridkin V M 2007 *Appl. Phys. Lett.* **90** 122904

[2] Park Y J, Kang S, Lotz B, Brinkmann M, Thierry A, Kim K and Park C 2008 *Macromolecules* **41** 8648

[3] Kang S J, Bae I, Park Y, Park T, Sung J, Yoon S, Kim K, Choi D and Park C 2009 *Adv. Funct. Mater.* **19** 1609

[4] Taylor G W, Burns J R, Kammann S M, Powers W B and Welsh T R 2001 *IEEE J. Oceanic Eng.* **26** 539

[5] Che B, Zhou X, Ren K, Neese B, Lin M, Wang Q, Bauer F and Zhang Q M 2006 *Science* **313** 334

[6] Granstrom J, Feenstra J, Sodano H A and Farinholt K 2007 *Smart Mater. Struct.* **16** 1810

[7] Yuan Y, Reece T J, Sharma P, Poddar S, Ducharme S, Gruverman A, Yang Y and Huang J 2011 *Nature Mater.* **10** 296

[8] Kochervinskii V V 2003 *Crystallogr. Rep.* **48** 649

[9] Poulsen M and Ducharme S 2010 *IEEE Trans. Dilectr. Electr. Insul.* **17** 1028

[10] Gruverman A, Auciello O and Tokumoto H 1998 *Annu. Rev. Mater. Sci.* **28** 101

[11] Balke N, Bdikin I, Kalinin S V and Kholkin A L 2009 *J. Am. Ceram. Soc.* **92** 1629

[12] Kim Y, Kim W, Choi H, Hong S, Ko H, Lee H and No K 2010 *Appl. Phys. Lett.* **96** 012908

[13] Colchero J, Storch A, Luna M and Go´mez Herrero J Baro A M 1998 *Langmuir* **14** 2230

[14] Freund J, Halbritter J and Horber J K H 1999 *Microscopy Res. Tech.* **44** 327

[15] Choi Y, Hong J, Hong S, Song H, Cheong D and No K 2010 *Phys. Status Solidi. RRL* **4** 94

[16] Weeks B L and Vaughn M W 2005 *Lanmuir* **21** 8096

[17] Dahan D, Molotskii M, Rosenman G and Rosenwaks Y 2006 *Appl. Phys. Lett.* **89** 152902

[18] He D Y, Qiao L J and Volinsky A A 2011 *J. Appl. Phys.* **110** 074104

[19] He D Y, Qiao L J, Volinsky A A, Bai Y, Wu M and Chu W Y 2011 *Appl. Phys. Lett.* **98** 062905

[20] Brugere A, Gidon S and Gautier B 2011 *J. Appl. Phys.* **110** 052016

[21] Kim K J, Reynolds N M and Hsu L 1989 *Macromolecules* **22** 4395

[22] Xia F, Razavi B, Xu H, Cheng Z Y and Zhang Q M 2002 *J. Appl. Phys.* **92** 3111

[23] Woo J, Hong S, Setter N, Shin H, Jeon J-U, Park Y E and No K 2001 *J. Vac. Sci. Technol.* B **19** 818

[24] Gruverman A, Kholkin A, Kingon A and Tokumoto H 2001 *Appl. Phys. Lett.* **78** 2751

[25] Hong J, Song H, Hong S, Shin H and No K 2002 *J. Appl. Phys.* **92** 7434

[26] Park M, Choi Y-Y, Kim J, Hong J, Song H W, Sung T-H and No K 2012 *Soft Matter* **8** 1064

[27] Sharma P, Nakajima T, Okamura S and Gruverman A 2013 *Nanotechnology* **24** 015706

[28] Jesse S *et al* 2008 *Nature. Mater.* **7** 209

[29] Sharma P, Reece T J, Ducharme S and Gruverman A 2011 *Nano Lett.* **11** 1970

[30] Light T S, Licht S, Bevilacqua A C and Morash K R 2005 *Electrochem. Solid-State Lett.* **8** E16

[31] Kim Y, Cho Y, No K, Hong S, Bühlmann S, Park H, Min D-K and Kim S-H 2006 *Appl. Phys. Lett.* **89** 162907

[32] Rodriguez B J, Jesse S, Baddorf A P, Kim S H and Kalinin S V 2007 *Phys. Rev. Lett.* **98** 247603

[33] Catalan G, Bea H, Fusil S, Bibes M, Paruch P, Barthelemy A and Scott J F 2008 *Phys. Rev. Lett.* **100** 027602

[34] Paruch P, Giamarchi T and Triscone J M 2005 *Phys. Rev. Lett.* **94** 197601